# CHAPTER VII

# CORRELATION OF VISCOSITY RATIO, MORPHOLOGY, AND MECHANICAL PROPERTIES OF POLYAMIDE 12/NATURAL RUBBER BLENDS VIA REACTIVE COMPATIBILIZATION

## 7.1 Abstract

Natural rubber (NR)-modified polyamide 12 (Nylon12/NR) was produced by melt blending Nylon12 and NR in the presence of polystyrene/maleated natural rubber (PS/MNR) copolymer as a reactive compatibilizer. The influence of compatibilizer loading on viscosity ratio, morphology, and mechanical properties of the blends was investigated. As a consequence of the reactive blend between Nylon12 and maleated NR in PS/MNR, the formation of amide and succinimide linkages was set at rubber-Nylon12 interfaces. Thus the dispersion of rubber particles was improved, and the particle coalescence was prevented so that the fine morphology with good interfacial adhesion was stabilized. This also resulted to enhance the blend viscosity and to lower viscosity ratio. The data revealed strong correlation between low viscosity ratio and fine spherical morphology of the compatibilized blends. An optimum PS/MNR compatibilizer content was at 7 phr to produce good dispersion of small rubber domains (size ≤ 0.3 micron) in Nylon12 matrix. Thermal properties by DSC revealed that crystallization temperature of Nylon12 was lowered by the presence of NR and crystallinity of Nylon12 was slightly affected by the PS/MNR content. An enhancement of mechanical properties, especially the impact energy was observed without suffering the tensile and flexural properties. Compared to the neat Nylon12, the compatibilized blends showed an increase in impact energy by a factor of 5. This large enhancement is successfully interpreted in term of the toughening effect by rubber phase of suitable dispersed size and the interparticle distance.

**Keywords:** Polyamides, Rubber, Compatibilization, Viscosity, Morphology, Mechanical Properties

## 7.2 Introduction

The production of tough materials often begins by incorporating elastomeric materials to rigid thermoplastic polymers. Polyamide is an engineering plastic of high strength but its limited use at low temperature due to increasing brittleness is major concern for a number of applications [1]. Toughening polyamide by incorporating several rubber materials has been studied for years. This research work considered modification of polyamide 12 (Nylon12) with natural rubber (NR) and its derivative as a reactive compatibilizer (PS/MNR). Nylon12 is a semicrystalline polymer and possesses longer hydrocarbon chains than any other commercially available polyamides; it thus offers flexibility with low melting temperature and very little moisture absorption (important to maintain high strength of Nylon). Accordingly, components made from Nylon12 show high degree of dimensional stability with high strength even in environments with fluctuating humidity levels. For example a bullet-proof vest, it is generally used to prevent bullet penetration; however, the bullet's energy is not vanished but transferred to and absorbed by the vest and the wearer who is then injured as blunt force trauma. Even without penetration, modern pistol bullets contain enough energy to cause blunt force trauma under the impact point. Hence, it would be better for a bullet-proof vest to be made of high impact resistance materials in order to prevent the blunt force trauma e.g. rubber-toughened Nylon12. Natural rubber (NR), a renewable biopolymer, is certainly capable to improve toughening properties of high performance plastics. Moreover, incorporating NR to toughen Nylon12 is appropriate in several considerations e.g. long hydrocarbon structure and low melting temperature of Nylon12 can provide some degree of compatibility and low temperature processing with NR. However, the incompatibility between Nylon12 and natural rubber due to poor polymer-rubber interactions or mismatched polarity at the interfaces remains a concern for achieving good mechanical properties. As seen in the work of Tanrattanakul et al. [2], incorporating 30 wt% NR in high strength Nylon 6 caused a 50% drop in yield strength without improvement in impact strength while using 30 wt% epoxidized natural rubber, the impact strength enhanced largely almost 6 times to 34.5 kJ/m$^2$ but with the expense of large 72% drop in yield and tensile strengths. They explained that it was attributed to poor morphology of wide

distribution of relatively large dispersed rubber size. It is imperative to note that a reactive compatibilizer must be used to promote interfacial adhesion between the blend components and to stabilize the blend morphology. In this work, we finally show that the appropriated morphology (uniformly fine dispersion) for good mechanical properties (especially toughness) can be developed and stabilized from the mixing step where the low viscosity ratio plays the crucial role to allow the minimum dispersed phase size as a consequence of the good interfacial adhesion formed by the reaction between functional groups of the blend components.

The reactive compatibilization technique has been widely used because it is fast, easy, and cost effective [3-5]. The copolymers functionalized with maleic anhydride (MA) are used as reactive compatibilizers in polyamide blend systems since the terminal amino groups of polyamide can react with the anhydride groups of compatibilizers to generate block or graft copolymers. These interactions enhance the interfacial adhesion between the blend components, leading to improved mechanical properties. Wilkinson *et al.* [6] revealed that the impact strength of PP/PA6/SEBS blends was increased by using SEBS-g-MA as the reactive compatibilizer. Axtell *et al.* [7] found that charpy impact strength of PA6/NR blend were improved when maleic anhydride modified natural rubber (NR-g-MA) was used as a third component in the blends. Similar results were found by Kim *et al.* for toughening Nylon 6 using ethylene-octene copolymer grafted with MA and styrene [8]. Our previous work studied Nylon12/NR blend compatibilized with polystyrene/natural rubber copolymer (PS/NR) [9]. The results indicated that this non-reactive compatibilizer acted as the efficient compatibilizer for Nylon12/NR blend, leading to the enhancement of mechanical properties. To increase the interfacial adhesion between Nylon12 and NR phases; hence, we studied preparation of polystyrene/maleated natural rubber copolymer (PS/MNR) for further used as a reactive compatibilizer for Nylon 12/NR blend to improve mechanical properties [10].

Generally, the improvement of mechanical properties including tensile, flexural, and impact properties is related to appropriate phase morphology. The morphology of polymer blends is created during mixing and is also affected by the viscosity ratio of the blend components ($\lambda$), the ratio of viscosity of dispersed phase

($\eta_d$) and the viscosity of continuous phase ($\eta_c$) [11]. For a particular binary blend, the viscosity of different components may show differences in sensitivity to temperature. Thus changing mixing temperature may affect the developed morphology of the blend e.g. ellipsoidal, spherical, or fibrillar domains [12]. In general, the dispersed phase assumes spherical domains for viscosity ratio closer to one. Few research studies demonstrate that the smallest particles of the dispersed phase are generated when the viscosity ratio is near unity, resulting in good mechanical properties [13,14]. Recently, Bucknall and Paul [15] reported that the tensile strength also depended on particles size and volume fraction of rubber phase. The small size rubber phase gave the highest tensile strength due to the strong resistance to cavitation. The relation of the dispersed phase size and the blend viscosity by considering a term involving phase composition was reported by Serpe et al. [16], and the dispersed phase diameter D can be calculated as shown in Equation (7.1).

$$D = \frac{4\sigma_{cd}(\eta_d / \eta_b)^{\pm 0.84}}{\gamma\,\eta_b[1 - (4\phi_d\phi_c)^{0.8}]} \qquad (7.1)$$

where $\sigma_{cd}$ is the interfacial tension between the dispersed phase and the continuous phases, $\eta_b$ is the viscosity of the blend, $\gamma$ is the shear rate, and $\phi_d$ and $\phi_c$ are the volume fraction of the dispersed phase and the continuous phase, respectively. The exponent in Equation (7.1) is positive for $\lambda > 1$ and negative for $\lambda < 1$. From Equation (7.1), it is clearly seen that the dispersed particle size is directly related to the viscosity ratio of the blends. The impact strength; however, is more dependent on the rubber content although the relationship between rubber content and the dispersed phase rubber particle size is not uniquely established. It is known that small rubber size of the order of 0.3 μm is critical to provide the highest impact strength [17].

The size of rubber domains changed with viscosity ratio (or compatibilizer content) within 0.2-0.6 μm which was about the size that exhibited the most significant toughening effect for several polyamide/rubber blends as found by several researchers, especially Wu in 1988 [18]. Kayano et al. [1] found that additional energy dissipation mechanism for fracture toughness corresponding to high impact strength was due to

plastic deformation around the crack tip leading to shear yielding and rubber cavitation. Wu [19] also found that besides uniform dispersion, the interparticle distance or matrix ligament thickness became a single parameter for explaining the toughening of the rubber filled plastic blend where the minimum good phase adhesion was presented. The matrix ligament allows shear yielding (in addition to rubber cavitation) due to the localized microscopic plane strain-plane stress transition. Thus it plays important role in determining the mechanical properties especially tensile modulus and toughness of the rubber-toughened plastics. The interparticle distance ($D_{ip}$), surface-to-surface distance between two nearest rubber particles, is directly proportional to the dispersed rubber phase diameter (D) and the reciprocal volume fraction of rubber ($\phi_r$) as reported by Wu's model in Equation (7.2).

$$D_{ip} = D\left[\left(\frac{\pi}{6\phi_r}\right)^{1/3} - 1\right] \qquad (7.2)$$

On the basis of above considerations, it is important that the rubber domains should have small particles to obtain rubber-toughened polyamides. Natural rubber-modified Nylon12 (Nylon12/NR) was prepared in this work by melt blending in an internal mixer, and the functional graft copolymer of polystyrene/maleated natural rubber (PS/MNR) was used as a reactive compatibilizer. We report the obvious improvement in mechanical properties including tensile and impact properties of the blends at various compatibilizer contents (while the flexural properties were slightly improved) could be controlled by lowering the viscosity ratio such that the fine scale rubber particles could be formed and stabilized by the formation of amide and succinimide linkages at the interface as a product from reactions between maleated NR in PS/MNR and amine groups in Nylon12. The correlation of the viscosity ratio, the phase morphology and the mechanical properties of the compatibilized blends are discussed in terms of dispersed particles size and the interparticle distance [18-20]. It is important to note that this achievement in enhancing the impact energy was easily obtained by using small amount of a reactive compatibilizer without the expense of the large drop in tensile and flexural properties.

## 7.3 Experimental

### 7.3.1 Materials

Polyamide 12 (PA12, Nylon12), grade Grilamid® L25 natural, was supplied by EMS-Chemie (Sumter, South Carolina). The melting temperature ($T_m$) and melt flow index (275 °C, 5 kg) of the polymer were 179 °C and 20 g/10 min, respectively. The polymer was available in pellet forms with the density of 1.09 g/cm$^3$. Natural rubber (NR) grade STR 5L with density of 0.93 g/cm$^3$ was purchased from Banpan Research Laboratory (Thailand) in yellow solid bulk form. Polystyrene/maleated natural rubber (PS/MNR) blend used as a reactive compatibilizer was prepared in our laboratory. The composition of the reactive compatibilizer was 60 wt% of PS and 40 wt% of MNR.

### 7.3.2 Preparation of Reactive Compatibilizer

Polystyrene/maleated natural rubber (PS/MNR) copolymer was prepared by using two-step mixing. In the first step, masticated NR was introduced in the internal mixer (Prep-Mixer®, C.W. Brabender, USA) and mixed for 3 min at a temperature of 135 °C and a rotor speed of 60 rpm. Then, 3 wt% of maleic anhydride (MA) was incorporated into rubber and further mixed for 5 min. Finally, the maleated natural rubber (MNR) was removed from the chamber. In the second step, the chamber temperature was increased up to 170 °C for melting PS at the rotor speed of 60 rpm. Then, 0.5 wt% of dicumyl peroxide (DCP) was added and mixed for 3 min. Finally, MNR was added to the molten PS and mixed for 4 min. The obtained blend is termed PS/MNR in the rest of the paper.

### 7.3.3 Preparation of [Nylon12/NR]/[PS/MNR] Blends

First, the chamber temperature and the rotor speed of the internal mixer were set at 210 °C and 70 rpm, respectively. Nylon12 (80 wt%) was fed into the chamber and allowed to melt for 3 min. Masticated NR (20 wt%) and PS/MNR were then added and mixed for another 4 min. PS/MNR copolymer with various contents of 1-10 phr (parts per hundred resin based on the total mass of Nylon12 and NR) was

used as a reactive compatibilizer for Nylon12/NR blend. By this procedure, the reaction between the anhydride groups of PS/MNR compatibilizer and the terminal amino groups of Nylon12 took place during mixing. It led to the formation of the intermediate amide linkages due to the nucleophilic attack of the amino groups on the carbonyl carbon of the anhydride groups. The thermal imidization reaction then occurred at a temperature above 100 °C. This reaction provides the succinimide linkages that tie the two phases of Nylon12 and NR together as shown in Scheme 7.1. The [Nylon12/NR]/[PS/MNR] blends are termed the compatibilized blends (C-Blends) in the rest of the paper.
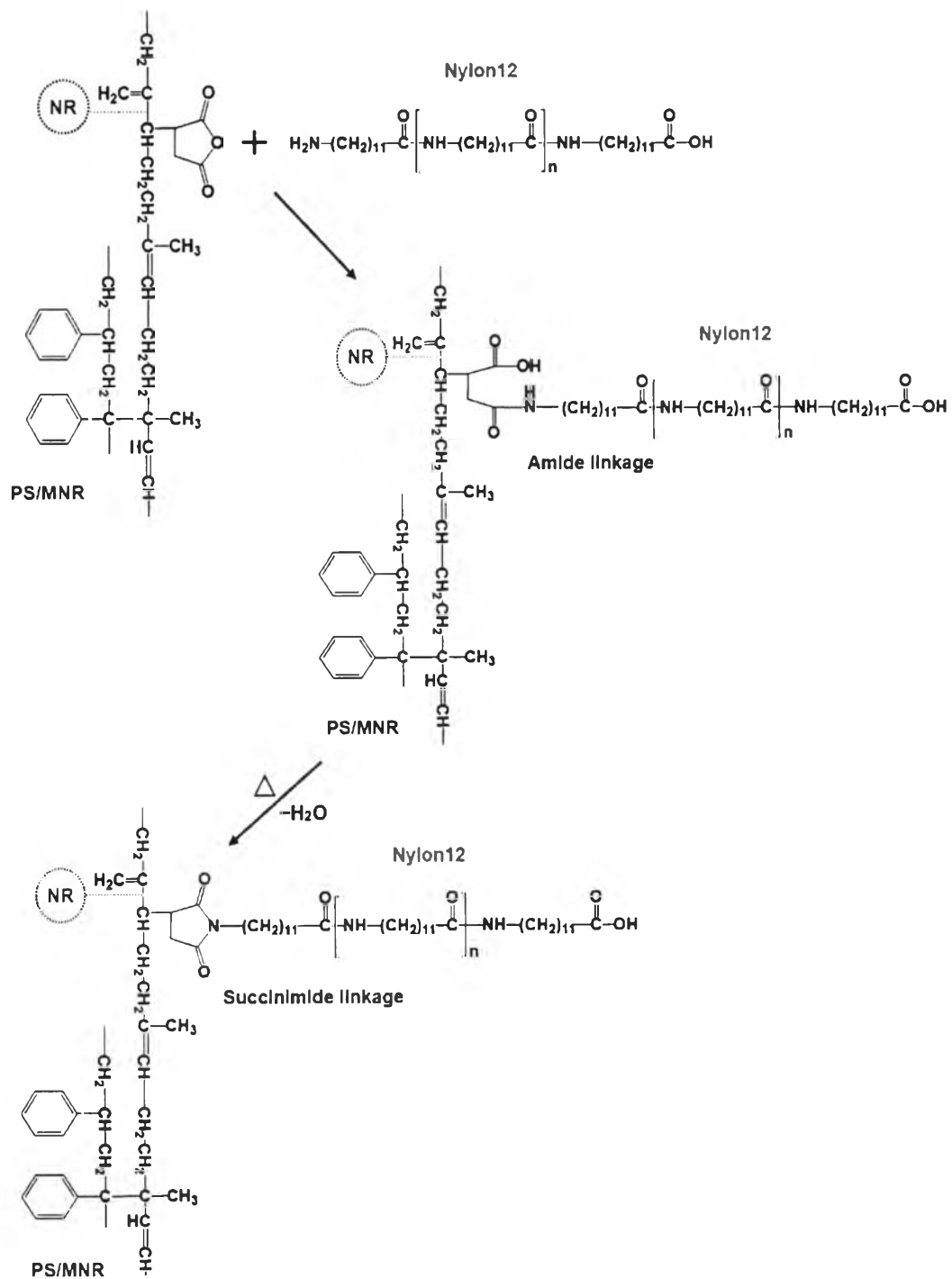
**Scheme 7.1** Formation of amide and succinimide linkage at Nylon12/NR interface via imidization reaction.

### 7.3.4 Viscosity Measurement

A twin-bore capillary rheometer (Rosand RH7, Malvern Instruments, USA) with bore diameter of 15 mm and bore length of 290 mm was used to measure the viscosity of the compatibilized blends. The length-to-inner diameter (L/D) ratio of the capillary die was 32/1. All measurements were made at a test temperature of 210 °C (processing temperature) and the range of apparent shear rates varied from 10 to 500 $s^{-1}$.

### 7.3.5 Phase Morphology

A scanning electron microscope (SEM, JEOL JSM-7401, USA) was used at 10 kV for two magnifications of 5,000 and 10,000 times (at scale of 1 $\mu$m) to investigate the morphology of the cross-sectional surface after sputtered coating by silver. For the preparation of the cross-sectional surface, all samples were cryogenically broken after dipping in liquid nitrogen for 15 min and then the dispersed rubber phase was removed by etching with mixed solvent of toluene (90 wt%) and isopropanol (10 wt%) for at least 3 days at 100 °C to get complete dissolution.

### 7.3.6 Thermal Analysis

Crystallization parameters were measured by using differential scanning calorimeter (DSC Q2000, TA Instruments, USA). The samples were heated from -20 to 210 °C at 10 °C/min in order to eliminate any thermal history of the material, and then, cooled from 210 to -20 °C at a rate of 5 °C/min. The samples were then heated from -20 to 210 °C at a rate of 10 °C/min. All these steps were carried out in a dry nitrogen atmosphere in order to avoid any possible thermal degradation. The peak temperatures of the corresponding exothermal and endothermal curves were taken as the crystallization temperature ($T_c$) and the melting temperature ($T_m$), respectively, and normalized by the weight of the sample. The degree of crystallinity ($\chi_c$) was calculated as seen in Equation (7.3).

$$\chi_c = \frac{\Delta H_b}{w\,\Delta H_0} \times 100 \tag{7.3}$$

where w was weight fraction of Nylon12 (0.73-0.8), $\Delta H_b$ was the enthalpy of fusion (area under the endotherm) of Nylon12 in the blends, and $\Delta H_0$ was the enthalpy of fusion for a 100% crystalline Nylon12 which was taken to be 245.69 J/g [21].

### 7.3.7 Tensile Test

A universal testing machine (Instron 5567, USA) with a crosshead speed of 10 mm/min and a load cell of 10 kN was used to measure the tensile properties, such as Young's modulus, tensile stress at yield, and elongation at break of the compatibilized blends. Tensile specimens (Type IV) were obtained from mini-injection molding with a specimen length of 60 mm, a gauge length of 32 mm, and a thickness of 3 mm. At least ten specimens were used for each blend to determine an average and standard deviation according to ASTM D638 at room temperature. Tensile toughness defined as the resistance to fracture of the materials under stress was then determined by integrating the stress-strain curve in unit of Joule per cubic metre ($J/m^3$) as shown below:

$$U_T \quad = \quad \text{Area underneath the stress–strain } (\sigma-\varepsilon) \text{ curve}$$
$$U_T \quad = \quad \sigma \times \varepsilon$$
$$U_T \quad = \quad \text{MPa} \times \%$$
$$U_T \quad = \quad (N \cdot m^{-2} \cdot 10^6) \times (m \cdot m^{-1} \cdot 10^{-2})$$
$$U_T \quad = \quad N \cdot m \cdot m^{-3} \cdot 10^4$$
$$U_T \quad = \quad J \cdot m^{-3} \cdot 10^4$$
$$U_T \quad = \quad kJ \cdot m^{-3} \cdot 10$$

where $U_T$ is the tensile toughness unit. Hence, the tensile toughness is calculated from multiplying the integrated area by 10 and is expressed in unit of $kJ/m^3$.

### 7.3.8 Flexural Test

A universal testing machine (Instron 4206, Thailand) was used to measure the flexural properties, e.g., flexural modulus, flexural stress at yield, and flexural strain of the compatibilized blends. Samples were obtained from compression molding with a depth of 3 mm, a width of 25 mm, and a length of 80 mm. All specimens were tested according to ASTM D790 (Three point bending) with a

crosshead speed of 2 mm/min, load cell of 5 kN, and support span of 50 mm. Five specimens were used for each sample to determine an average and standard deviation.

### 7.3.9 Impact Test

The impact energy of the compatibilized blends with various PS/MNR contents is expressed in energy lost per unit of thickness (J/m). All specimens were prepared by using DSM mini-injection molder with a length of 60 mm, a thickness of 3 mm, and a width of 12 mm. The specimens were then V-notched on the center of one longitudinal side, providing a width of 10.2 mm under notch. The impact test was done by using an impact tester (Model No.43-1, Testing Machines Inc., USA) according to ASTM D256 with the pendulum 40.6 J (30 ft·lbs) at room temperature. At least ten specimens were used for each sample to determine an average and standard deviation.

## 7.4 Results and Discussion

### 7.4.1 Viscosity Ratio and Estimation of Dispersed Phase Size

In polymer blends, dispersed phase droplet formation under shear follows elongation into a thread or ellipsoid or cylinder depending on the viscosity and volume fraction of the phases. These elongated domains undergo breakup during melt mixing due to the imbalance between interfacial and viscous forces. The particle size and the particle shape of the dispersed phase are also controlled by the viscosity ratio. Generally, the droplet formation in the shear field is limited to the viscosity ratio of less than 3.5 [22], and the smallest particle size of the dispersed phase is achieved when the viscosity ratio is close to unity.

Figure 7.1 shows the double logarithmic plot of relationship between shear viscosity and shear rate for neat Nylon12, NR, PS/MNR(compatibilizer), Nylon12/NR binary blend (noncompatibilized blend, B-Blend) and [Nylon12/NR]/[PS/MNR] blends (reactive compatibilized blends, C-Blend) with various compatibilizer contents. These materials showed pseudo-plastic behaviour from an evident reduction of shear viscosity with increasing shear rate. The viscosity ratios calculated from the ratio of the dispersed phase (NR) viscosity to the continuous

phase (Nylon12) viscosity ($\eta_d/\eta_c$) and the ratio of the dispersed phase viscosity to the blend viscosity ($\eta_d/\eta_b$) are also shown in Figure 7.2.
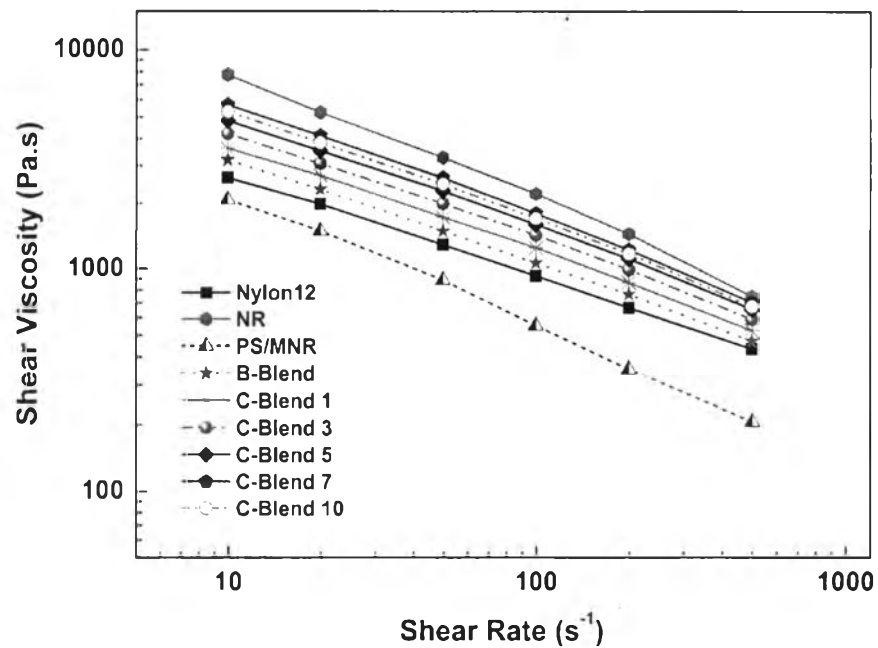


**Figure 7.1** Shear viscosity *versus* Shear rate for neat Nylon12, NR, PS/MNR, B-Blend and C-Blends with various compatibilizer contents.
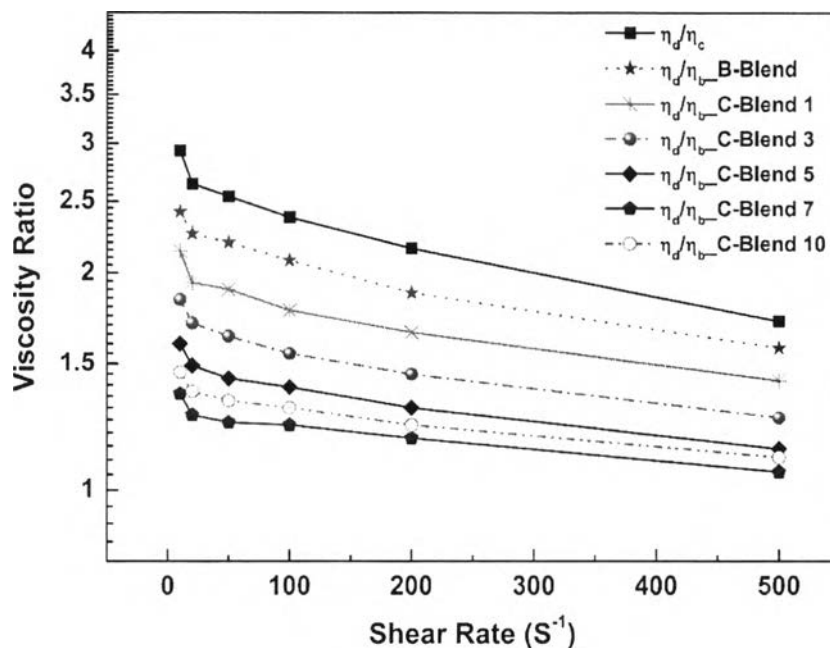
**Figure 7.2** Viscosity ratios calculated from the ratio of the dispersed viscosity to the continuous viscosity ($\eta_d/\eta_c$) and the ratio of the dispersed viscosity to the blend viscosity ($\eta_d/\eta_b$) with various compatibilizer contents and shear rates.

The results revealed that the viscosity ratio of the compatibilized blends at any shear rates was lower than that of the binary blend (noncompatibilized blend), and reduced with an increase of the compatibilizer content up to 7 phr. This suggested that the presence of reactive compatibilizer helped to increase the interfacial adhesion at the Nylon12/NR interfaces via the formations of amide and succinimide linkages, as described by Sathe *et al.* and Roeder *et al.* [23,24]. These interactions produced the bulky structure (see Scheme 7.1) and rendered rigidity to molecular chains that in turn, resisted the flow or increased the viscosity. Moreover, the reactions developed and stabilized fine particle dispersion morphology in solid state. This is clearly attributed to the presence of amide and succinimide linkages at the interface to prevent the coalescence of rubber particles and to provide good interfacial adhesion. The more amount of PS/MNR supply more linkages enough to cover and stabilize the smaller rubber particles. From these results, the estimated size (diameter) of the dispersed rubber phase of the compatibilized blends with various compatibilizer contents and at

different shear rates can be calculated by using Equation (7.1) and tabulated in Table 7.1. The values of other parameters used in Equation (7.1) was 2.08 mN/m for the interfacial tension of Nylon12/NR at the processing temperature of 210 °C [25], 0.23 for the volume fraction of the dispersed phase (NR), and 0.77 for the volume fraction of the continuous phase (Nylon12). The optimum content of PS/MNR was estimated at 7 phr where the minimum rubber diameter was obtained. It was obvious that PS/MNR composed of rubber; the excess amount of PS/MNR preferred to add in the rubber phase resulting in the increase in rubber particle diameter and lowering the blend viscosity.

Table 7.1 The dispersed phase diameter (μm) from calculation ($D_c$) of B-Blend and C-Blends with various compatibilizer contents (1-10 phr) and shear rates (10-500 s$^{-1}$)

| Shear Rate (s$^{-1}$) | Dispersed Phase Diameter from Calculation (μm) | | | | | |
| | B-Blend | C-Blend | | | | |
| | | 1 | 3 | 5 | 7 | 10 |
| --- | --- | --- | --- | --- | --- | --- |
| 10 | 2.26 | 1.80 | 1.36 | 1.06 | 0.79 | 0.89 |
| 20 | 1.47 | 1.11 | 0.88 | 0.68 | 0.51 | 0.59 |
| 50 | 0.89 | 0.68 | 0.52 | 0.41 | 0.31 | 0.39 |
| 100 | 0.60 | 0.45 | 0.35 | 0.28 | 0.23 | 0.25 |
| 200 | 0.38 | 0.30 | 0.24 | 0.19 | 0.16 | 0.17 |
| 500 | 0.21 | 0.18 | 0.14 | 0.12 | 0.10 | 0.11 |

The viscosities of the compatibilized blends increased leading to the lowering of their viscosity ratios. As a consequence, the rubber particle size was clearly reduced with shear rate and compatibilizer contents. Considering shear rate, the dispersed rubber phase diameter was approximately decreased by a factor of 10 with increasing shear rate from 10 to 500 s$^{-1}$ (50 times).

### 7.4.2 Phase Morphology of [Nylon12/NR]/[PS/MNR] Blends

During blend preparation using the internal mixer, the shear rate of mixing is related to the effective rotor dimension as reported by Goodrich and Porter [26], and can be calculated from Equation (7.4).

$$\gamma = 16\pi N \left[ \frac{\beta^2}{(1+\beta)^2(\beta^2-1)} \right] \approx \frac{2\pi N}{\ln\beta} \tag{7.4}$$

where N is the rotor speed in revolutions per second, and $\beta$ is the ratio of the radius of chamber ($R_e$) and the radius of the rotor ($R_i$).

The internal mixer with the capacity of 275 g pellet had $R_e$ of 30 mm and $R_i$ of 26 mm approximately [27]. Using the rotor speed of 70 rpm, the shear rate of the mixing chamber calculated from Equation (7.4) was approximately 50 s$^{-1}$. Hence, the diameter of the dispersed rubber phase calculated from Equation (7.1) at shear rate of 50 s$^{-1}$ was used to compare with the number averaged diameter of the dispersed phase. The latter was estimated from the average diameter of about 200 domains randomly selected from SEM micrographs.

Figures 7.3 and 7.4 show SEM micrographs in SEI mode of the cryo-fractured surfaces of the binary blend (noncompatibilized blend, B-Blend) and the ternary blend (compatibilized blends, C-Blends) with various compatibilizer contents at magnifications of 5,000 and 10,000 times, respectively. The binary blend with the highest viscosity ratio showed the ellipsoidal rubber domains due to the more predominant cohesive force of NR than the interfacial force. After addition of 1 phr PS/MNR reactive compatibilizer, the ellipsoidal rubber domains allowed the stretch-out of MA along the shear field and promoted its interaction with Nylon12.The force on the surface of the dispersed rubber phase exceeded the strength provided by its cohesive force. Consequently, the elongated particles broke and then formed spherical particles which were also a result of simultaneous lowering of the viscosity ratio. The higher amount of compatibilizer provided more interactions that were capable of breaking the rubber phase into smaller and smaller domains with more uniform diameter. The reacted species remained at the interfaces and stabilized the fine morphology.
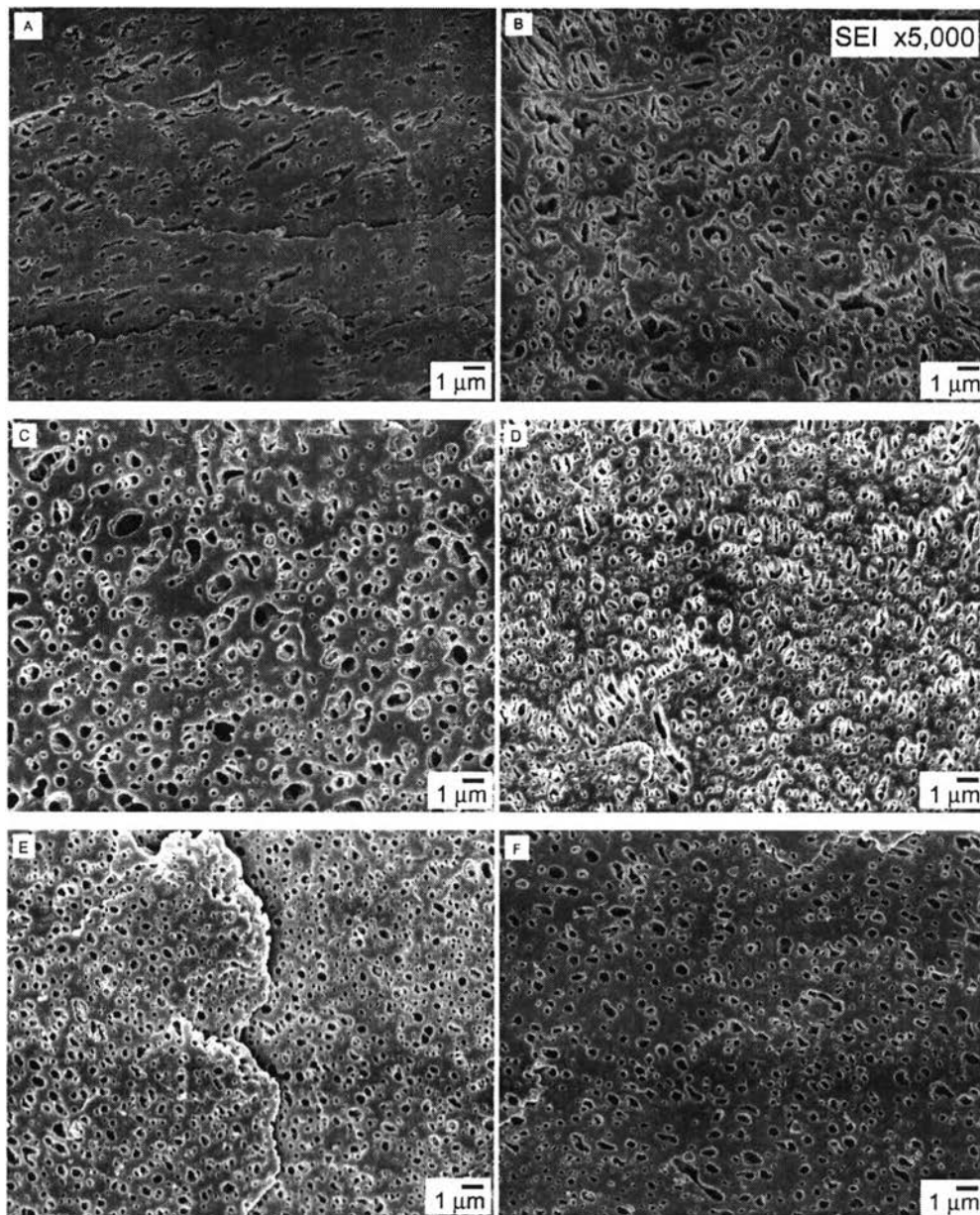
**Figure 7.3** SEM micrographs in SEI mode at magnification x5,000 and scale 1 μm of the C-Blends with compatibilizer content of (A) 0 phr, (B) 1 phr, (C) 3 phr, (D) 5 phr, (E) 7 phr, and (F) 10 phr.
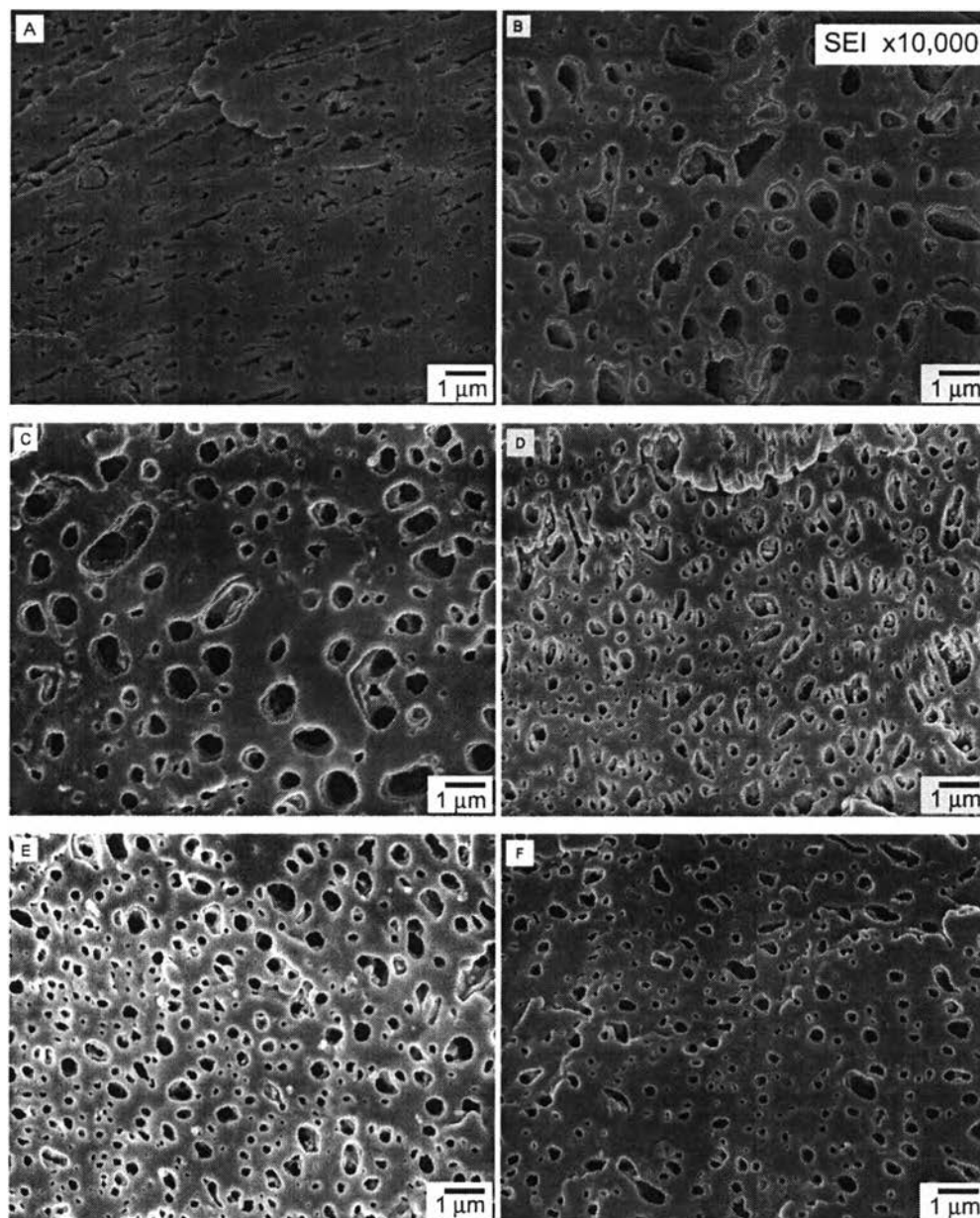
**Figure 7.4** SEM micrographs in SEI mode at magnification x10,000 and scale 1 μm of the C-Blends with compatibilizer content of (A) 0 phr, (B) 1 phr, (C) 3 phr, (D) 5 phr, (E) 7 phr, and (F) 10 phr.

The dispersed phase diameter (D) and the interparticle distance ($D_{ip}$) obtained both from calculation and from measurement are also shown in Table 7.2. The average diameters from measurement ($D_m$) of the dispersed phase were less than 1 μm and lower than the estimated diameters from calculation ($D_c$). This suggested that besides viscosity ratio that was altered by the compatibilizer content, the value of interfacial tension, shear rate, and the blend viscosity all exerted important influence on dispersion and the size of rubber particles. However, the discrepancy is minimized as the content of PS/MNR increases approaching the optimum value. At the optimum compatibilizer loading of 7 phr, the compatibilized blends showed the finest phase morphology with the dispersed phase diameter of 0.20 μm. It is clearly seen that the reactive compatibilization prevented the coalescence of rubber particles and improved the morphological stability of the compatibilized blends by the introduction of steric hindrance. This melt rheology and solid morphology correlation for good phase adhesion is thus achieved. Beyond this amount, when compatibilizer content of 10 phr was used, the rubber particle size increased to approximately 0.27 μm. This is attributed to the increase of low molecular weight NR content with an increase of the compatibilizer loading. From Figure 7.1, the viscosity of PS/MNR was in the range of 200-2,000 Pa.s depending on shear rate range of 10-500 $s^{-1}$ which was lower than that of Nylon12 and NR. This also indicates that the molecular weight of NR in the compatibilizer is shorter than that of neat NR. The low viscosity of the compatibilizer overwhelmed the stiffness of the succinimide linkages. The rubber domains became soft and thus grew in size. Accordingly, the extent of reaction of MA with Nylon12 at the interface became much less.

**Table 7.2** The dispersed phase diameter (D) and the interparticle distance ($D_{ip}$) from calculation (c) and measurement (m) of B-Blend and C-blends with various compatibilizer contents

| Materials | Dispersed Phase Diameter (μm) | | Interparticle Distance (μm) | |
|---|---|---|---|---|
| | $D_c$ | $D_m$ | $D_{ip,c}$ | $D_{ip,m}$ |
| B-Blend | 0.89 | 0.57 | 0.28 | 0.34 |
| C-Blend 1 | 0.68 | 0.44 | 0.21 | 0.22 |
| C-Blend 3 | 0.52 | 0.41 | 0.16 | 0.15 |
| C-Blend 5 | 0.41 | 0.22 | 0.13 | 0.12 |
| C-Blend 7 | 0.31 | 0.20 | 0.10 | 0.10 |
| C-Blend 10 | 0.39 | 0.27 | 0.12 | 0.14 |

It is clearly seen in Table 7.2 and Figure 7.5 (SEM micrograph in LEI mode) that the interparticle distance reduced with rubber particle diameter. It changed with the compatibilizer content in similar trend as the particle size. The measured interparticle distance values are 0.10-0.22 μm for the reactive compatibilized blends, in the same range as calculated and found by other [28-30], and 0.34 μm for the binary blend. So with the good interfacial adhesion, a thinner interparticle distance results in a greater transition of plane strain to plane stress giving higher toughness and higher elongation as mentioned by Wu [19].
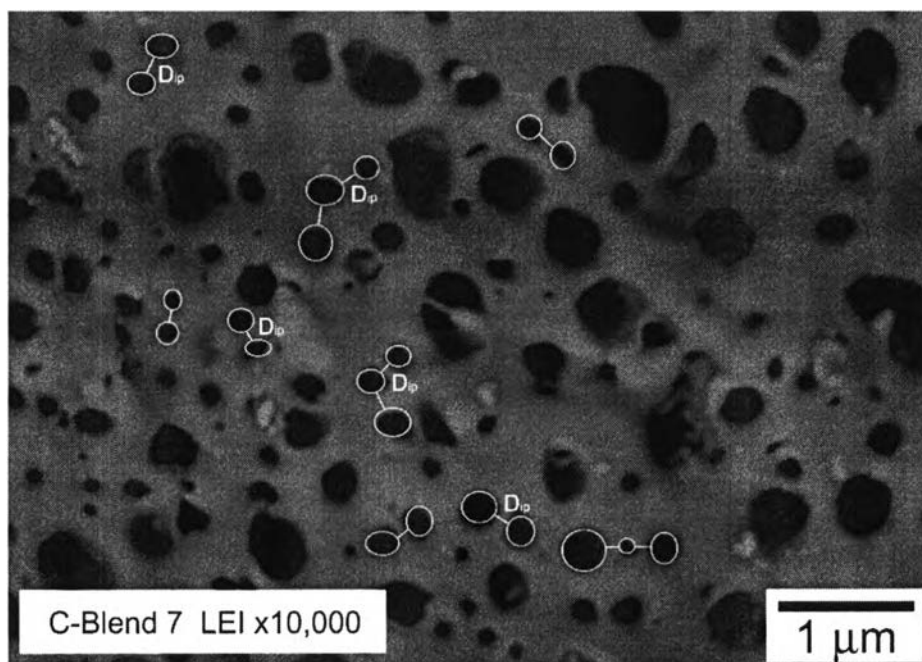
**Figure 7.5** SEM micrograph in LEI mode shows the dispersed rubber phase (circle) and the interparticle distance (straight line) of C-Blends at 7 phr PS/MNR.

### 7.4.3 Thermal Properties of [Nylon12/NR]/[PS/MNR] Blends

Thermal results in Table 7.3 demonstrate that the additions of NR and PS/MNR reactive compatibilizer into Nylon12 matrix had significant effect on the melting temperature ($T_m$) of Nylon12 and the reduction of the crystallinity ($\chi_c$) from 21 % for the neat Nylon12 to around 19.5-20.7 % for C-Blends. For Nylon12, the $\gamma$-phase crystal structure is the most common thermodynamically stable form and characterized as a triclinic structure with a typical melting temperature of 179 °C [31]. The addition of NR in the binary blend clearly showed the lowering in $T_m$ while the addition of PS/MNR in the reactive compatibilized blends led to the restoration of Nylon12 melting temperature. The later effect confirms that the reactive compatibilizer does not influence the melting of Nylon12 crystalline or the perfection of normal Nylon12 crystalline. On the other hand, the crystallinity of Nylon12 decreased slightly with the addition of NR (20.4 %) and further lowered gradually with high PS/MNR content. The incorporation of more flexible and amorphous NR together with good interfacial adhesion by the reactive compatibilization was able to interfere

the melt crystallization of Nylon12, as evident from the lowering of melt crystallization temperature ($T_c$) and also found in other works e.g. Nylon6/PP/PP-g-maleic anhydride blends [23]. Furthermore, due to compatibilizer containing short-chain NR, an increase in compatibilizer content also resulted in an increase of NR phase in the compounds.

**Table 7.3** Crystallization temperature ($T_c$), Melting temperature ($T_m$) and Crystallinity ($\chi_c$) of C-Blends with various compatibilizer contents

| Materials | $T_c$ (°C) | $T_m$ (°C) | $\Delta H_m$ (J/g) | $\chi_c$ (%) |
|---|---|---|---|---|
| Nylon12 | 149.5 | 177.8 | 52.1 | 21.2 |
| B-Blend | 148.4 | 177.8 | 40.1 | 20.4 |
| C-Blend 1 | 148.3 | 177.2 | 39.3 | 20.2 |
| C-Blend 3 | 147.5 | 178.3 | 39.1 | 20.5 |
| C-Blend 5 | 148.4 | 177.6 | 38.7 | 20.7 |
| C-Blend 7 | 147.6 | 177.8 | 36.2 | 19.7 |
| C-Blend 10 | 148.7 | 177.9 | 34.8 | 19.5 |

### 7.4.4 Mechanical Properties of [Nylon12/NR]/[PS/MNR] Blends

Mechanical properties of all samples were determined by tensile test, flexural test, and impact test. Stress-strain curves can be used to classify the materials into two broad categories; namely, the brittle materials and the ductile materials [32,33]. The brittle materials fracture at low strains and absorb little energy; conversely, the ductile materials fail after significant plastic strain (deformation) and absorb more energy. The stress-strain curves of neat Nylon12, the Nylon12/NR binary blend (B-Blend) and the compatibilized blends (C-Blends) with various compatibilizer contents (presented in Figure 7.6) demonstrate the ductile behavior of such blends.

The result shown in Figure 7.7 for the binary blend revealed that its tensile modulus reduced as compared to that of Nylon12, e.g. from 1240 MPa to 845

MPa. The tensile yield stress reduced from 47 MPa to 39 MPa while the elongation at break increased from 70 % to 84 % as shown in Figures 8 and 9, respectively. These are attributed to the dilution effect of rubber phase and the reduced crystallinity. Besides, the incompatibility between Nylon12 and NR resulted from the lack of specific interactions at their interfaces also caused the lowering of tensile properties. The modulus increased approximately to 900 MPa after a small amount (1-5 phr) of the reactive compatibilizer was added. At the optimum compatibilizer loading of 7 phr, the modulus (1194 MPa) and yield stress (47 MPa) of the reactive blend dramatically increased to about the same values as those of the neat Nylon12 but with almost twice the elongation at break of Nylon12. The softening of the reactive compatibilized blend (lowering of modulus and yield stress) is obvious after further increase of compatibilizer content (up to 10 phr); the increased content of low MW rubber phase in compatibilizer results in weakened mechanical strengths while the elongation was not affected. It is also seen in Figure 7.10 that an increase of tensile stress and elongation at break led to the enhancement of tensile toughness from 29,140 kJ/m$^3$ for neat Nylon12 to maximum 55,530 kJ/m$^3$ for the compatibilized blend containing 7 phr PS/MNR.

Flexural properties such as flexural modulus, flexural stress at yield, and flexural strain at break of neat Nylon12, B-Blend and C-Blends with various PS/MNR contents are also shown in Figures 7.7-7.9, respectively. As compared to Nylon12, the flexural modulus and the flexural strength of both B-Blend and C-Blends reduced while their flexural strain increased slightly when NR was incorporated into Nylon12 matrix, similar to what was seen earlier for tensile properties. The flexural modulus was found to decrease from 520 MPa for neat Nylon12 to 360 MPa for the noncompatibilized blend (Nylon12/NR binary blend, B-Blend) due to the incompatibility between Nylon12 phase and NR phase. However, the flexural modulus of the compatibilized blends (C-Blends) increased up to approximately 420 MPa when the reactive compatibilizer was added to the system. For the flexural stress at yield, the compatibilized blends showed the higher values (~ 26 MPa) when compared to the noncompatibilized blend (~ 14 MPa). The flexural strain (at break) for all samples was within 11-12.8 % where the reactive blends gave the intermediate values about 12 %. Considering an influence of compatibilizer content on flexural properties, it shows

insignificant strengthening effect. The flexural strength is rather a minor indicator for toughening that is developed with an optimum compatibilizer content [23].
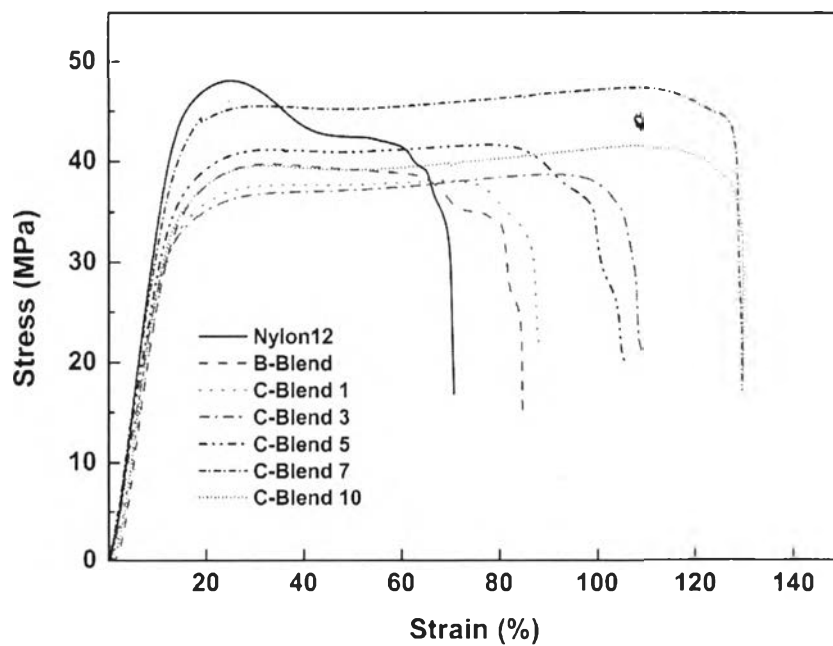


**Figure 7.6** Stress-Strain curves of neat Nylon12, B-Blend and C-Blends with various compatibilizer contents.
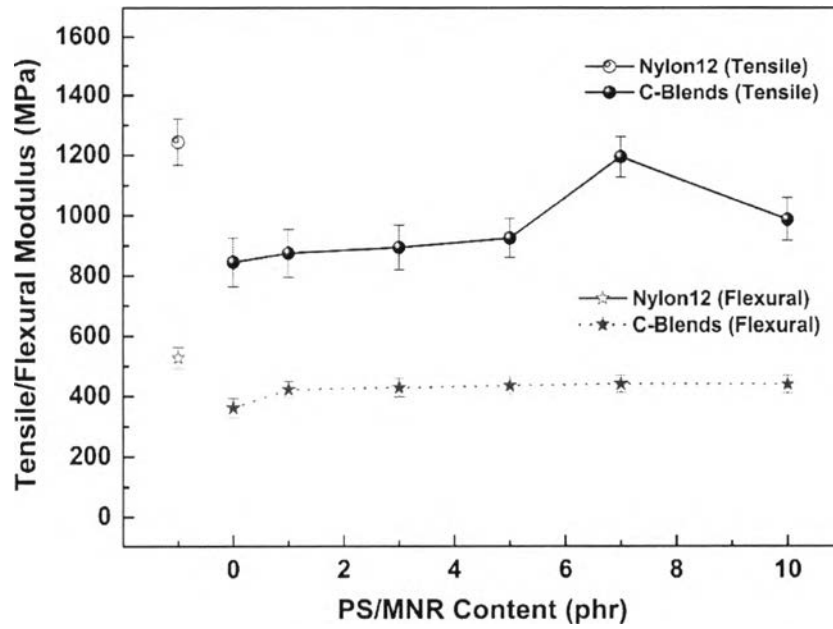
**Figure 7.7** Tensile and flexural modulus of neat Nylon12 and C-Blends with various compatibilizer contents.
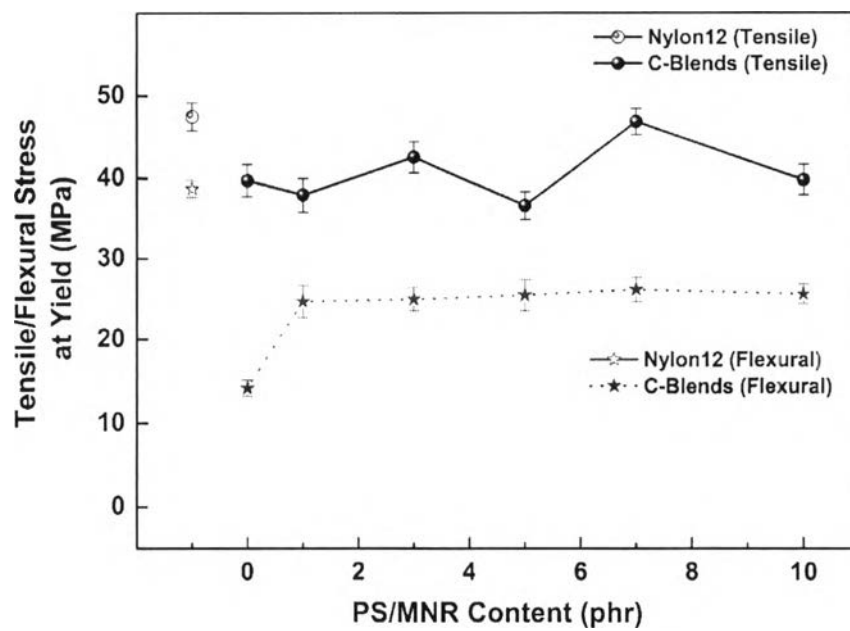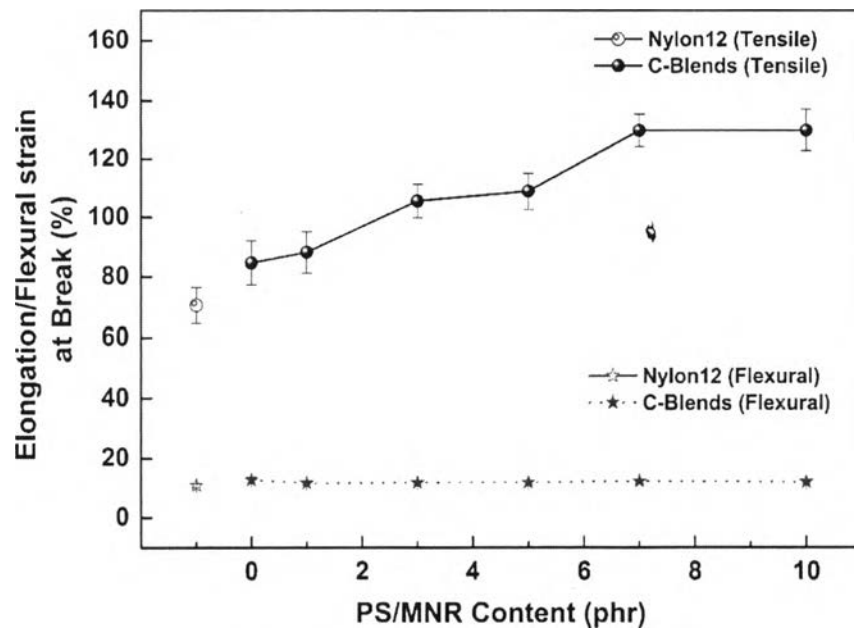


**Figure 7.8** Tensile and flexural stress at yield of neat Nylon12 and C-Blends with various compatibilizer contents.

**Figure 7.9** Elongation and flexural strain at break of neat Nylon12 and C-Blends with various compatibilizer contents.
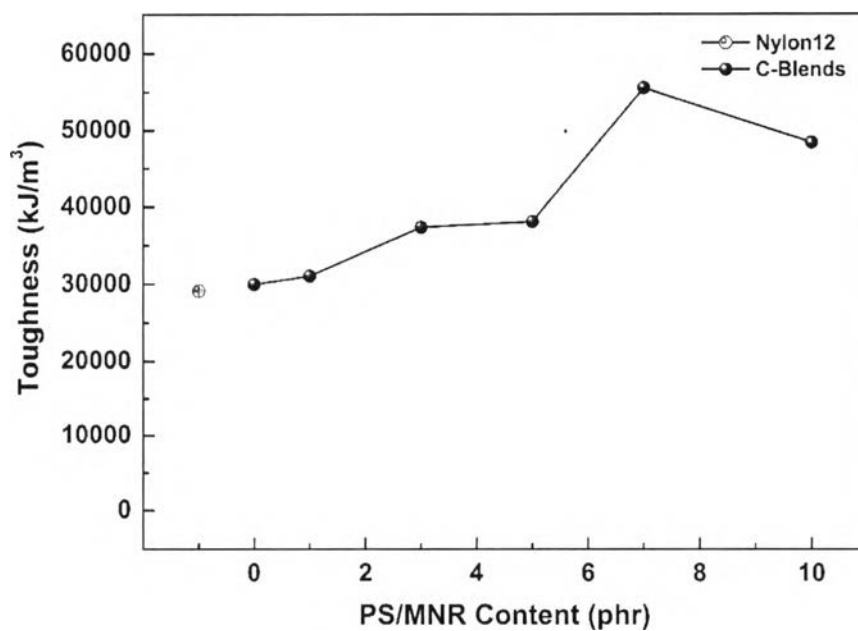


**Figure 7.10** Tensile toughness of neat Nylon12 and C-Blends with various compatibilizer contents.

Similar to tensile toughness, the impact results in Figure 7.11 show that the incorporation of NR favors the toughness enhancement of Nylon12. The impact energy of the binary blend increased largely to 241 J/m (approximately twice that of neat Nylon12), resulting from rubber promoting energy absorption. With adding reactive compatibilizer, the impact energy further increased up to 503 J/m for the compatibilized blends containing 7 phr of PS/MNR. This suggests that the interfacial adhesion via the formation of succinimide linkages at Nylon12/NR interfaces was significantly strong and allowed better energy transfer from Nylon12 matrix to NR phase and more energy dissipation mechanisms. Besides good adhesion of the small rubber domains, the interparticle distance also played an important role on the toughening efficiency of rubber-modified polyamides for interparticle distance less than 0.3 $\mu$m [18]. Figures 7.12 and 7.13 reveal that the increase in impact energy and toughness of ductile polymers such as polyamides also correlates with the reduction of rubber particle size and interparticle distance [18-20,34]. Borggreve *et al.* [35] showed that the brittle-tough transition temperature of Nylon6/EPDM-g-MA blend reduced with decreasing interparticle distance. At room temperature (~ 30 °C), the Nylon6/EPDM-g-MA blend was tough when the interparticle distance of EPDM phase was 0.3 $\mu$m approximately. In our case, a small interparticle distance allows large plastic deformation of Nylon12 matrix, promoting toughness of the compatibilized blends.

From these results, it is clearly seen that PS/MNR blend was an efficient compatibilizer for the incompatible blend Nylon12/NR. This successful strengthening and toughening improvement of Nylon12 cannot disregard the attribution to the presence of amide and succinimide linkages (produced from the imidization reaction). These chemical linkages increased the interfacial adhesion at Nylon12/NR interfaces as evident by an increase in the blend viscosity, leading to develop fine rubber particles and proper interparticle distance. In this work as shown in Table 7.2 and Figure 7.5, the smallest average particle size together with the thinnest interparticle distance is found in the compatibilized blend containing 7 phr of PS/MNR (C-Blend 7) as compared with other blends. The stabilized phase morphology of fine dispersion ensures an increase of interfacial interaction and adhesion between the two phases. This along with the suitable interparticle distance leads to dramatic increase in

toughening by energy dissipation mechanisms, i.e. plane strain to plane stress transition and shear yield propagation as suggested by Wu [18]. In addition, the reactive blends contained less crystallinity; this is preferential for an increase of impact resistance because the amorphous part of the materials is free structure which can be altered to alleviate the imposed energy (better energy absorption than crystalline).
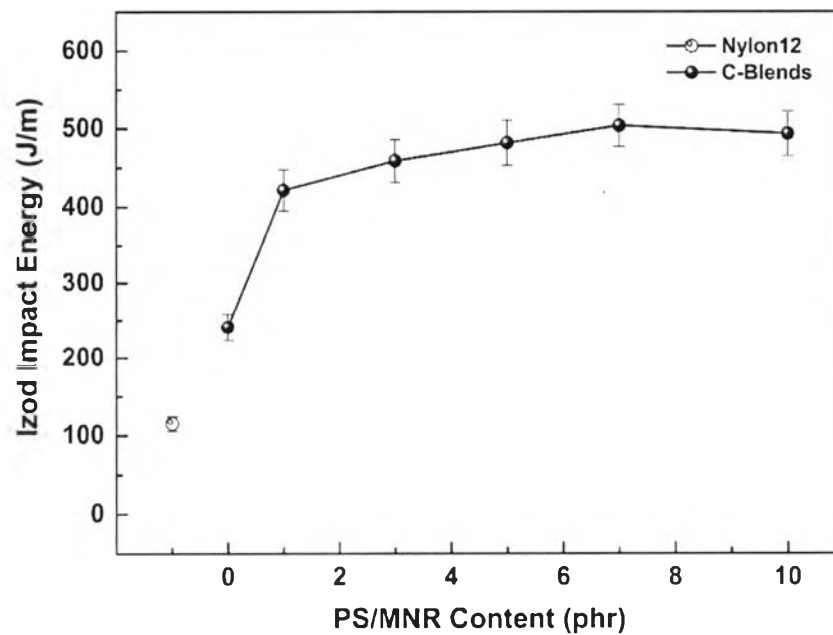


**Figure 7.11** Impact energy (J/m) of neat Nylon12 and C-Blends with various compatibilizer contents.
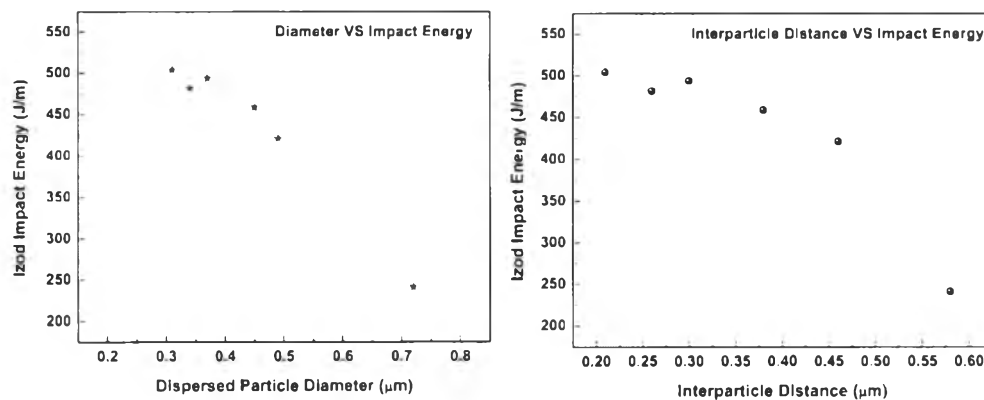
**Figure 7.12** Effect of dispersed phase diameter and interparticle distance on Izod impact energy.
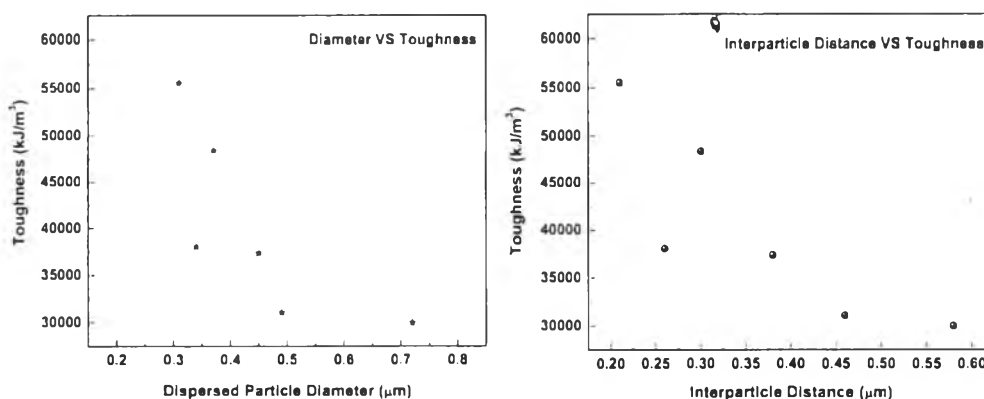


**Figure 7.13** Effect of dispersed phase diameter and interparticle distance on tensile toughness.

## 7.5 Conclusions

Natural rubber-modified Nylon12 (Nylon12/NR) for application demanding high impact resistance and low moisture absorption was prepared by melt blending process using a graft copolymer of polystyrene and maleated natural rubber (PS/MNR) as a reactive compatibilizer. The correlation of viscosity ratio and morphology affecting mechanical properties of the blends was then investigated. The results illustrated that the use of reactive compatibilizer gave an effective compatibilization

for Nylon12/NR blend (at composition of 80:20 wt%) so that mechanical properties (both tension and toughening) were significantly improved. The increasing of PS/MNR content results in reducing viscosity ratio in melt state to achieve a finely dispersed rubber phase as well as improving mechanical properties in solid state. Especially at the optimum content (7 phr) of the PS/MNR compatibilizer, the compatibilized blend shows significant improved in toughening with impact energy almost 5 times that of Nylon12 while retaining the original Nylon12 tensile properties but with twice elongation at break. The flexural modulus of this optimum compatibilized blend was just slightly less from the neat Nylon12. During mixing, the reactive compatibilization yielded amide and succinimide chemical linkages that resulted to increase the blend viscosity and reduce the viscosity ratio closed to one such that the dispersed rubber phase prefers to break into smaller droplets. The amide and succinimide linkages residing at the interface could suppress the coalescence of rubber particles during mixing in the melt state due to the steric hindrance of its bulky structure. Hence, it provided more stable and better blended phase morphology. In other words, the reactive compatibilizer controls viscosity ratio to support drop break-up process and simultaneously forms a bulky interfacial linkages and good interfacial adhesion that stabilize phase morphology for good energy transfer and to be in the properly small size and interparticle distance for more energy dissipation mechanisms. This leads to the improvement of mechanical properties and toughening at the same time. Thermal properties informed the decrease in crystallization temperature and crystallinity of Nylon12 with the addition of NR while the variation of PS/MNR content mainly resulted to reduce crystallinity of Nylon12.

## 7.6 Acknowledgements

## 7.7 References

1.  Kayano Y, Keskkula H, Paul DR (1998) Fracture behaviour of some rubber-toughened nylon 6 blends. Polymer 39:2835-2845.

2.  Tanrattanakul V, Sungthong N, Raksa P (2008) Rubber toughening of nylon 6 with epoxidized natural rubber. Polym Test 27:794-800.

3.  Groeninckx G, Harrats C, Thomas S (2001). In: Baker WE, Scott CE, Hu GH (eds) Reactive Polymer Blending. Hanser, Munich.

4.  Kitayama N, Keskkula H, Paul DR (2000) Reactive compatibilization of nylon 6/styrene–acrylonitrile copolymer blends. Part 1. Phase inversion behavior. Polymer 41:8041-8052.

5.  Koning C, Van Duin M, Pagnoulle C, Jerome R (1998) Strategies for compatibilization of polymer blends. Prog Polym Sci 23:707-757.

6.  Wilkinson AN, Laugel L, Clemens ML, Harding VM, Marin M (1999) Phase structure in polypropylene/PA6/SEBS blends. Polymer 40:4971-4975.

7.  Axtell FH, Phinyocheep P, Kriengchieocharn P (1996) The effect of modified natural rubber compatibilizers on polyamide6/natural rubber blends. J Sci Soc Thailand 22:201-216.

8.  Kim JG, Lee J, Son Y (2014) Toughening of nylon 6 with an ethylene–octene copolymer grafted with maleic anhydride and styrene. Mater Lett 126:43-47.

9.  Saengthaveep S, Magaraphan R (2013) Natural rubber–toughened Nylon12 compatibilized by polystyrene/natural rubber blend. Adv Polym Tech 32:1-11.

10. Saengthaveep S, Jana SC, Magaraphan R Natural Rubber-Toughened Polystyrene: Effects of Mixing Procedure and Maleic Anhydride Content on Impact Property and Phase Morphology Proceedings of Multi-Functional Materials and Structures IV, Bangkok, Thailand. pp 607-610.

11. Taylor GI The formation of emulsions in definable fields of flow. Proceedings of The Royal Society A: Mathematical, physical & Engineering Science. pp 501-523.

12. Cheng Z, Wang Q (2006) Morphology control of polyoxy-methylene/thermoplastic polyurethane blends by adjusting their viscosity ratio. Polym Int 55:1075-1080.

13.  Mbarek S, Jaziri M, Chalamet Y, Carrot C (2010) Effect of the viscosity ratio on the morphology and properties of PET/HDPE blends with and without compatibilization. J Appl Polym Sci 117:1683-1694.

14.  Hietaoja PT, Holsti-Miettinen RM, Seppälä JV, Ikkala OT (1994) The effect of viscosity ratio on the phase inversion of polyamide 66/polypropylene blends. J Appl Polym Sci 54:1613-1623.

15.  Bucknall CB, Paul DR (2013) Notched impact behaviour of polymer blends: Part 2: Dependence of critical particle size on rubber particle volume fraction. Polymer 54:320-329.

16.  Serpe G, Jarrin J, Dawans F (1990) Morphology-processing relationships in polyethylene-polyamide blends. Polym Eng Sci 30:553-565.

17.  Huang JJ, Keskkula H, Paul DR (2004) Rubber toughening of an amorphous polyamide by functionalized SEBS copolymers: morphology and Izod impact behavior. Polymer 45:4203-4215.

18.  Wu S (1988) A generalized criterion for rubber toughening: The critical matrix ligament thickness. J Appl Polym Sci 35:549-561.

19.  Wu S (1990) Chain structure, phase morphology, and toughness relationships in polymers and blends. Polym Eng Sci 30:753-761.

20.  Wu S (1985) Phase structure and adhesion in polymer blends: A criterion for rubber toughening. Polymer 26:1855-1863.

21.  Pyda M (2013). In: Piorkowska E, Rutledge GC (eds) Handbook of polymer crystallization. John Wiley, New Jersey.

22.  Grace HP (1982) Dispersion phenomena in high viscosity immiscible fluid systems and application of static mixers as dispersion devices in such systems. Chem Eng Commun 14:225-277.

23.  Sathe SN, Devi S, Rao GSS, Rao KV (1996) Relationship between morphology and mechanical properties of binary and compatibilized ternary blends of polypropylene and nylon 6. J Appl Polym Sci 61:97-107.

24.  Roeder J, Oliveira RVB, Gonçalves MC, Soldi V, Pires ATN (2002) Polypropylene/polyamide-6 blends: influence of compatibilizing agent on interface domains. Polym Test 21:815-821.

25. Magaraphan R, Totanapoka C, Jamieson AM (2004) Morphology of Nylon12/natural rubber blends compatibilized by reactive processing. Des Monomers Polym 7:165-180.

26. Goodrich JE, Porter RS (1967) A rheological interpretation of torque-rheometer data. Polym Eng Sci 7:45-51.

27. Bousmina M, Ait-Kadi A, Faisant JB (1999) Determination of shear rate and viscosity from batch mixer data. J Rheol 43:415-433.

28. Huang JJ, Keskkula H, Paul DR (2006) Comparison of the toughening behavior of nylon 6 versus an amorphous polyamide using various maleated elastomers. Polymer 47:639-651.

29. Oshinski AJ, Keskkula H, Paul DR (1996) The role of matrix molecular weight in rubber toughened nylon 6 blends: 2. Room temperature Izod impact toughness. Polymer 37:4909-4918.

30. Oshinski AJ, Keskkula H, Paul DR (1992) Rubber toughening of polyamides with functionalized block copolymers: 1. Nylon-6. Polymer 33:268-283.

31. Li L, Koch MHJ, Jeu WHd (2003) Crystalline structure and morphology in nylon-12: A small- and wide-angle X-ray scattering study. Macromolecules 36:1626-1632.

32. Beer F, Johnston R, Dewolf J, Mazurek D (2009) Mechanics of materials McGraw-Hill, New York.

33. Faker M, Razavi Aghjeh MK, Ghaffari M, Seyyedi SA (2008) Rheology, morphology and mechanical properties of polyethylene/ethylene vinyl acetate copolymer (PE/EVA) blends. Eur Polym J 44:1834-1842.

34. Borggreve RJM, Gaymans RJ, Luttmer AR (1988) Influence of structure on the impact behaviour of nylon-rubber blends. Makromol Chem-M Symp 16:195-207.

35. Borggreve RJM, Gaymans RJ, Schuijer J, Housz JFI (1987) Brittle-tough transition in nylon-rubber blends: effect of rubber concentration and particle size. Polymer 28:1489-1496.